Available online at www.sciencedirect.com

ScienceDirect

Chinese Journal of Aeronautics 23(2010) 341-350

Chinese Journal of Aeronautics

www.elsevier.com/locate/cja

Study on UAV Path Planning Approach Based on Fuzzy Virtual Force

Dong Zhuoning[a,*], Zhang Rulin[b], Chen Zongji[a], Zhou Rui[a]

[a]*School of Automation Science and Electrical Engineering, Beijing University of Aeronautics and Astronautics, Beijing 100191, China*

[b]*Flight Automatic Control Research Institute, Xi'an 710065, China*

Received 3 June 2009; accepted 16 October 2009

Abstract

This article proposes a novel fuzzy virtual force (FVF) method for unmanned aerial vehicle (UAV) path planning in complicated environment. An integrated mathematical model of UAV path planning based on virtual force (VF) is constructed and the corresponding optimal solving method under the given indicators is presented. Specifically, a fixed step method is developed to reduce computational cost and the reachable condition of path planning is proved. The Bayesian belief network and fuzzy logic reasoning theories are applied to setting the path planning parameters adaptively, which can reflect the battlefield situation dynamically and precisely. A new way of combining threats is proposed to solve the local minima problem completely. Simulation results prove the feasibility and usefulness of using FVF for UAV path planning. Performance comparisons between the FVF method and the A* search algorithm demonstrate that the proposed approach is fast enough to meet the real-time requirements of the online path planning problems.

Keywords: fuzzy virtual force; unmanned aerial vehicle; path planning; hybrid system; Bayesian belief network; fuzzy logic reasoning; local minima

1. Introduction

Path planning is one of the fundamental issues in unmanned aerial vehicle (UAV) research. A standard path planning problem is to determine an optimal or feasible path in time between desired locations under specific constraints. After path planning, UAVs have the ability to penetrate threats of enemy, accomplish specific tasks in enemy's air defense area and assure their safety.

In previous research, there are several path planning algorithms for UAVs that attract much attention, such as the A* searching algorithm[1], the Voronoi diagram search method[2], the dynamic programming[3], the bionic algorithm[4] and so on. In literature, UAV path planning is widely studied and applied. Particularly, in recent years, Y. Kim, et al.[5] proposed real-time path planning schemes employing limited information for fully autonomous UAVs in a hostile environment. C. L. Bottasso, et al.[6] presented another novel planning strategy for high performance aggressive autonomous UAVs, in which the smoothing step optimizes a given trajectory expressed in terms of a sequence of waypoints and connecting straight trim flight conditions.

However, all the above algorithms cause huge computational cost, especially in a complicated environment or in a large searching space. Therefore, these algorithms cannot meet the real-time requirements of path planning.

In order to solve the problems mentioned above, virtual force (VF) method was proposed, which was firstly designed for mobile robot obstacle avoidance, so that a robot could move swiftly and placidly among the obstacles[7-8]. The main idea of the VF method is to regard a robot as a particle in a three-dimensional space where the robot moves under the VF. The VF function is defined as the superposition of the attractive force from target and the repulsive force from obstacles. The most prominent advantage of the VF method is its simplicity and the high ability of real-time computation.

However, the path planning based on VF still has some limitations:

(1) The category of threats defined by repulsion force is not enough and the setting of parameters is not

*Corresponding author. Tel.: +86-10-82339993.
E-mail address: dongzhuoning@buaa.edu.cn
Foundation items: National Natural Science Foundation of China (60975073); Aeronautical Science Foundation of China (2008ZC13011); Research Foundation for Doctoral Program of Higher Education of China (20091102110006); Fundamental Research Funds for the Central Universities

doi: 10.1016/S1000-9361(09)60225-9

systematic.

(2) The planning space is not partitioned reasonably and the path is not smoothed during the planning process.

(3) Technical principles are hard to be verified because of the lack of integrated mathematical descriptions.

(4) As the path planning is a process of steepest gradient descent, the inherent disadvantages of the VF method are local minima and vibration.

At present, there is an extensive literature on solving the local minima problem of the VF method, the majority of which uses either of the following three solutions when applying the VF method to robotics: assistant force[9-10], virtual obstacle[11] or sub-goal[12]. However, all of these solutions are only applicable in simple or singular situations while none of them can solve the local minima problem completely. In order to apply the VF method to UAV path planning problems, this limitation should be eliminated thoroughly.

In our previous work[13], several types of threats were defined. The planning space was partitioned according to the mission constraints, the path was flyable by UAVs and the constraint condition of the parameters in the path planning method was verified.

This article mainly focuses on a novel UAV path planning approach using fuzzy virtual force (FVF). Specifically, an integrated mathematical description to the UAV path planning and the optimal solving method under a given cost function are presented. To meet the real-time requirements of online UAV path planning, fixed step length is used in iteration. The adaptive proportion coefficient based on the Bayesian belief network and fuzzy logic reasoning is applied. Finally, the combination of threats is proposed for solving the local minima problem.

2. Modeling of VF based UAV Path Planning

The UAV path planning is a process that we assume a virtual UAV moves continuously along a particular path from a fixed starting point to a given destination. The VF based path planning is then a process where the change of path direction is decided by the direction of the VF. Therefore, the VF based path planning can be regarded as an optimal control problem in a discrete-continuous hybrid system, where the movement is continuous and the change of direction is discrete. In this hybrid system, the final state is fixed because of the given destination, and the terminal time is unknown.

The main purpose for this hybrid system control is to solve the optimization problem as to when to switch the path direction with the lowest cost.

The evolution of the hybrid system can be expressed as follows:

$$\begin{bmatrix}\dot{x}\\ \dot{y}\end{bmatrix}=U_1\begin{bmatrix}1\\0\end{bmatrix}+U_2\begin{bmatrix}0\\1\end{bmatrix}+U_3\begin{bmatrix}\sqrt{2}/2\\ \sqrt{2}/2\end{bmatrix}+U_4\begin{bmatrix}-\sqrt{2}/2\\ \sqrt{2}/2\end{bmatrix}+U_5\begin{bmatrix}\sqrt{2}/2\\ -\sqrt{2}/2\end{bmatrix} \quad (1)$$

where the state variables x and y are the coordinates of the planned point; U_i (i = 1,2,⋯,5) represents the discrete inputs taking the values of $\{0,v\}$, where v represents the velocity of the virtual UAV in the path planning process. Based on our previous work[13], U_i can be defined by $U_i = g(x, y, \Phi, \Delta)$, where Φ is the total amount of threats and Δ is the position of the destination.

We can also define the cost function as

$$J = a\int_T \Phi v \mathrm{d}t + b\Gamma \quad (2)$$

where a and b represent the weights of the path cost and the turning cost, respectively, Γ is the turning frequency. If the direction of the virtual UAV has been changed for s times in the path planning process, the main problem of the optimal control in this hybrid system is to find an appropriate discrete time sequence $T = [\tau_0,\tau_1], [\tau_1,\tau_2], [\tau_2,\tau_3],\cdots,[\tau_{s-1},\tau_s]$, in order to minimize the cost function of Eq.(2). τ_j (j = 1,2,⋯, s) is the time point of direction change and $[\tau_{j-1},\tau_j]$ is the time duration of the virtual UAV moving in the same direction.

2.1. Hybrid system model

Using the Alur-Courcoubetis-Henzinger-Ho (ACHH) model[14], the hybrid automaton is described as $A_{\mathrm{ACHH}}=(V_{\mathrm{D}},Q,\mu_1(Q),\mu_2,\mu_3)$, where

(1) Data variable $V_{\mathrm{D}} = \{x(t),y(t)\}$ is the set of positions of planned points with respect to the time t.

(2) Location Q = {1,2,3,4,5} represents the finite set of states corresponding to the planned direction.

(3) Activities:

$$\mu_1(1)\rightarrow\begin{bmatrix}\dot{x}\\ \dot{y}\end{bmatrix}=v\begin{bmatrix}1\\0\end{bmatrix} \quad (3)$$

$$\mu_1(2)\rightarrow\begin{bmatrix}\dot{x}\\ \dot{y}\end{bmatrix}=v\begin{bmatrix}0\\1\end{bmatrix} \quad (4)$$

$$\mu_1(3)\rightarrow\begin{bmatrix}\dot{x}\\ \dot{y}\end{bmatrix}=v\begin{bmatrix}\sqrt{2}/2\\ \sqrt{2}/2\end{bmatrix} \quad (5)$$

$$\mu_1(4)\rightarrow\begin{bmatrix}\dot{x}\\ \dot{y}\end{bmatrix}=v\begin{bmatrix}-\sqrt{2}/2\\ \sqrt{2}/2\end{bmatrix} \quad (6)$$

$$\mu_1(5)\rightarrow\begin{bmatrix}\dot{x}\\ \dot{y}\end{bmatrix}=v\begin{bmatrix}\sqrt{2}/2\\ -\sqrt{2}/2\end{bmatrix} \quad (7)$$

(4) Location invariant:

$$\mu_2\rightarrow\left\{M_{\min}\le J=a\int_T\Phi v\mathrm{d}t+b\Gamma\le M_{\max}\right\} \quad (8)$$

where $M_{\min}$ and $M_{\max}$ represent the boundary value of cost.

(5) Transition relation:

$$\mu_3\rightarrow\{J=M_{\max},U_i=g(x,y,\Phi,\Delta)\} \quad (9)$$

There are several constraints in UAV path planning problems such as minimum step length, path distance constraint, maximum turning angle, etc. The solutions should satisfy the above constraints in detail.

Minimum step length ($L_{\min}$):

$$L_{\min} < (\tau_{j+1} - \tau_j)v \tag{10}$$

Path distance constraint ($L_{\max}$):

$$\int_T v \cdot \mathrm{d}t < L_{\max} \tag{11}$$

Given activities ($\mu_1(1),\mu_1(2),\cdots,\mu_1(5)$), we can guarantee that the maximum turning angle condition will be satisfied.

2.2. Optimal solving method

The solutions for the above model are described as follows:

Step 1 Define the real-time cost $J_{\mathrm{rt}} = \sum_j \Phi \Delta d_j$, and set the current point as the starting point, where Δd_j represents the unit distance.

Step 2 Compute J_{rt} of the current point.

Step 3 When $J_{\mathrm{rt}} \geq M_{\max}$ and $(\tau_{i+1}-\tau_i)v > L_{\min}$, set the corresponding planned point as the current point, re-compute the mapping direction of the composition of VF.

Step 4 Repeat Steps 2-3 until the destination is reached.

Step 5 Compute $J = a\sum J_{\mathrm{rt}} + b\Gamma$ and $\int_T v \cdot \mathrm{d}t$, and change the value of $M_{\max}$. Repeat Steps 1-4 until $M_{\max}$ and the corresponding planned path, which is the optimal path under given J, are obtained.

3. FVF Method for UAV Path Planning

In order to meet the real-time requirements of the UAV path planning, the optimal solving method needs further improvement. In this section, FVF method combining VF and fuzzy logic reasoning is proposed to adapt to the complicated environment.

FVF method includes three components: fixing the iteration step to reduce computational cost, applying the Bayesian belief network and fuzzy logic reasoning to set the path planning parameters adaptively, and combining threats to avoid local minima.

3.1. Fixed step method

As the optimal solving method is a variable step length optimization, it cannot suit the real application because of its huge computational cost. Instead of variable step length, fixed step length is used in iteration.

The attractive forces are as follows:

$$\left.\begin{aligned} F_{\mathrm{A}x} &= G_{\mathrm{A}} \cos(\theta_{\mathrm{A}}) / R_{\mathrm{A}}^2 \\ F_{\mathrm{A}y} &= G_{\mathrm{A}} \sin(\theta_{\mathrm{A}}) / R_{\mathrm{A}}^2 \end{aligned}\right\} \tag{12}$$

where $F_{\mathrm{A}x}$ and $F_{\mathrm{A}y}$ are the attractive force projected to x and y axes respectively, G_{A} is a positive attractive force constant, R_{A} the distance between the current position and the destination, θ_{A} the angel between x axis and the line from the current point to the destination.

The repulsive forces can be expressed as

$$\left.\begin{aligned} F_{\mathrm{R}x} &= -G_{\mathrm{R}} \cos(\theta_{\mathrm{R}}) \mathrm{e}^{-R_{\mathrm{R}}/r_0} \\ F_{\mathrm{R}y} &= -G_{\mathrm{R}} \sin(\theta_{\mathrm{R}}) \mathrm{e}^{-R_{\mathrm{R}}/r_0} \end{aligned}\right\} \tag{13}$$

where $F_{\mathrm{R}x}$ and $F_{\mathrm{R}y}$ are the repulsive force projected to x and y axes, G_{R} is a positive repulsive force constant, R_{R} the distance between the current position and threat, r_0 a constant which can be set as the radius of threat, θ_{R} the angle between x axis and the line from the current point to threat. We define the proportion coefficient k by

$$k = G_{\mathrm{R}} / G_{\mathrm{A}} \tag{14}$$

The change of the coordinates Δx and Δy can be obtained by

$$\left.\begin{aligned} \Delta x &= \delta\alpha(F_{\mathrm{A}x} + \sum F_{\mathrm{R}x}) \\ \Delta y &= \delta\alpha(F_{\mathrm{A}y} + \sum F_{\mathrm{R}y}) \end{aligned}\right\} \tag{15}$$

where δ is the step length and

$$\alpha = [(F_{\mathrm{A}x} + \sum F_{\mathrm{R}x})^2 + (F_{\mathrm{A}y} + \sum F_{\mathrm{R}y})^2]^{-1/2} \tag{16}$$

The coordinates of the current position in the path planning process are updated according to Eq.(15).

In order to reach the given destination, the step length δ must meet Theorem 1 as follows.

Theorem 1 (Reachable Condition of Path Planning) In the path planning method based on VF, given $F_{\mathrm{R}x}=\beta_x F_{\mathrm{A}x}$, $F_{\mathrm{R}y}=\beta_y F_{\mathrm{A}y}$ and $\beta = \min(\beta_x,\beta_y)$, if the step length δ satisfies the inequality

$$\delta \leq H(1+\beta) \tag{17}$$

then, the condition $d \leq \Delta d$, $\Delta d \geq \delta$ must be satisfied after path planning iteration in finite steps, where H and Δd are the thresholds. When $d \leq \Delta d$, the path can reach the destination.

Proof Given the destination $G(x_{\mathrm{g}},y_{\mathrm{g}})$, the planned point after the Nth step P_N (x_N, y_N) as the current point and $x_{\mathrm{g}}-x_N \geq 0$, $y_{\mathrm{g}}-y_N \geq 0$, the distance between the destination and the current point satisfies

$$d_N^2 = (x_{\mathrm{g}} - x_N)^2 + (y_{\mathrm{g}} - y_N)^2 \tag{18}$$

and

$$|F_{\mathrm{A}}| = G_{\mathrm{A}} / R_{\mathrm{A}}^2 = G_{\mathrm{A}} / d_N^2 \tag{19}$$

$$|F_{\mathrm{A}x}| = \frac{x_{\mathrm{g}} - x_N}{d_N}|F_{\mathrm{A}}|, \quad |F_{\mathrm{A}y}| = \frac{y_{\mathrm{g}} - y_N}{d_N}|F_{\mathrm{A}}| \tag{20}$$

When the path goes along the direction of the VF with the step length δ, the position $P_{N+1}(x_{N+1},y_{N+1})$ after the (N+1)th step satisfies

$$\begin{aligned} x_{N+1} &= x_N + \delta\alpha(F_{Ax} + F_{Rx}) \\ y_{N+1} &= y_N + \delta\alpha(F_{Ay} + F_{Ry}) \end{aligned} \tag{21}$$

The distance between $P_{N+1}(x_{N+1},y_{N+1})$ and the destination is

$$d_{N+1}^2 = (x_g - x_{N+1})^2 + (y_g - y_{N+1})^2 \tag{22}$$

Substitute the values of F_{Ax}, F_{Ay} in Eq.(20) and x, y in Eq.(21) into Eq.(18) and Eq.(22), we get

$$\begin{aligned} d_{N+1}^2 - d_N^2 \le \delta^2 - 2\delta\alpha\left|F_A\right|(1+\beta)\cdot \\ [(x_g - x_N)^2 + (y_g - y_N)^2]/d_N \end{aligned} \tag{23}$$

Substituting the value of d_N in Eq.(18) into Eq.(23), we get

$$d_{N+1}^2 - d_N^2 \le \delta^2 - 2\delta\alpha\left|F_A\right|d_N(1+\beta) \tag{24}$$

Therefore, when inequality

$$\delta < 2\alpha\left|F_A\right|d_N(1+\beta) \tag{25}$$

is satisfied, $d_{N+1}^2 - d_N^2 < 0$. With the increase of planning steps, the path converges to the destination. Substituting Eq.(19) into Eq.(25), we get

$$\delta < 2\alpha G_A(1+\beta)/d_N \tag{26}$$

Set $H = 2\alpha G_A/d_{max}$, where d_{max} is the maximum of d_N, obviously $H > 0$. Therefore, when $\delta \le H(1+\beta)$, the reachable condition is satisfied.

When $\beta > -1$, Eq.(26) is solvable, which means that the total repulsive force is always smaller than the attractive force in all directions on every point in the path planning process.

If the selected step length violates the above limitation, the planning result will be irrational or even cannot reach the destination. On the other hand, it is obvious that the computational cost will increase remarkably if the step length is too short.

3.2. Adaptive proportion coefficient based on Bayesian belief network and fuzzy logic reasoning

According to the VF theory[4], the proportion coefficient k decides the risk-taking relations between the planned path and the given threats. The larger k in Eq.(14) results in a farther path away from threats; the smaller k results in a nearer path.

In the previous research, k is usually assigned according to trail-and-error experience. However, because of the battlefield environment, tactic requirements and the status information of UAVs are changing in real time; only the online awareness and reasoning can reflect the battlefield situation dynamically and precisely.

In order to obtain k adaptively, reasoning factors are chosen as

Factor 1 Performance capability level (PCL).

Factor 2 Time requirement (TmR).

PCL is defined to reflect holistic perception, comprehension and prediction of UAV's running state and performance capacity. PCL can be assessed using the Bayesian belief network.

(1) Bayesian belief network

Consider the Bayesian belief network model[15], where the node Z has q child nodes Y_1, Y_2, ⋯, Y_q and one parent node U. We introduce the following denotations:

Bel—Posterior probability distribution of Z.

λ—Diagnosis probability, reflecting the evident effect from the child nodes.

π—Casual probability, reflecting the casual effect from parent nodes and brother nodes.

$M_{Z|U}=P(Z|U)$—The conditional probability of a child node Z under a given parent node U.

The Bayesian belief network will be updated by the following three steps when the new knowledge comes.

Step 1 Update the local belief of the node itself:

$$\left.\begin{aligned} \mathrm{Bel}(z) &= \sigma\lambda(z)\pi(z) \\ \lambda(z) &= \prod_i \lambda_{Y_i}(z) \\ \pi(u) &= \pi_Z(u)M_{Z|U} \end{aligned}\right\} \tag{27}$$

Step 2 Update from the bottom up:

$$\lambda_Z(u) = \lambda(z)M_{Z|U} \tag{28}$$

Step 3 Update from the top down:

$$\pi_{Y_i}(z) = \sigma\pi(z)\prod_{j\ne i}\lambda_{Y_j}(z) \tag{29}$$

where $\pi_Z(u)$ is the casual predictive probability from node U to Z and $\lambda Y_i(z)$ the evident diagnosis support from the child node Y_i of Z. The unitary operator σ can ensure that $\sum_z \mathrm{Bel}(z) = 1$.

Using the Bayesian belief network above, PCL can be computed from the input information such as the vehicle states, weapon states, fuel information, and failure information. The Bayesian belief network model is illustrated in Fig.1.

(2) Fuzzy logic reasoning

Proportion coefficient k can be computed using fuzzy logic reasoning. The general format of the reasoning rules is shown in Table 1.

Mamdani method is used in fuzzy logic reasoning, and the centroid approach is used to defuzzify:

$$k = \left[\sum_{i=1}^n k_i\mu_K(k_i)\right] \Big/ \left[\sum_{i=1}^n \mu_K(k_i)\right] \tag{30}$$

where K represents a fuzzy set, $\mu_K(\cdot)$ is the membership function of k_i in K.

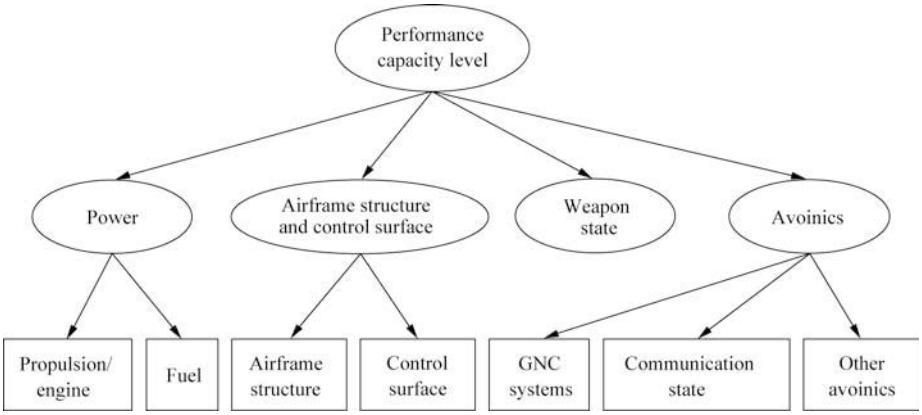

Fig.1 Bayesian belief network model for PCL.

Table 1 Fuzzy reasoning rules for solving proportion coefficient *k*

Rule number	Description
1	If TmR is low and PCL is weak, *k* is large
2	If TmR is low and PCL is strong, *k* is middle
3	If TmR is middle and PCL is middle, *k* is middle
4	If TmR is high and PCL is weak, *k* is middle
5	If TmR is high and PCL is strong, *k* is small

3.3. Avoiding local minima using combination of threats

The fundamental reason of the local minima problem in VF method is a concave distribution of virtual potential field. The VF can be obtained by the gradient of the virtual potential $\boldsymbol{W}$:

$$\boldsymbol{F}(\boldsymbol{x}) = -\nabla \boldsymbol{W}(\boldsymbol{x}) \tag{31}$$

It is obvious that, the VF at the point $\boldsymbol{x}$ is pointed to the center of the local minima region. Once the path enters the concave region, the path planning process has to be terminated.

The local minima problem can be described as follows: given the existing sets A and B, every element x_1 in A satisfies $f(x_1)\in B$ and every element x_2 in B satisfies $f(x_2)\in A$. The union of A and B forms the local minima area where $f(\cdot)$ represents the path planning process. The description of local minima is presented in Fig.2.

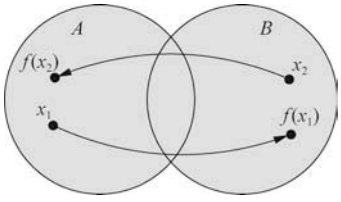

Fig.2 Description of local minima.

To determine whether the path planning process is trapped in a local minima area, the following two criteria are used.

Criterion 1 $|\boldsymbol{F}_N|=0$ and the path has not reached the destination.

Criterion 2 $\boldsymbol{F}_N = -\boldsymbol{F}_{N+1}$ and the path has not reached the destination.

To overcome the local minima problem, the combination of threats is proposed. When the threats that cause the concave distribution are combined to form one threat, the virtual potential field can be turned into a protruding distribution according to Eq.(31). The path planning process can escape from local minima successfully because the region has higher potential than its surrounding configurations. Therefore, the principle of threats combination is to eliminate the concave distribution.

The definition of distance d_{Threat} between any two threats is given as

$$d_{\text{Threat}} = \frac{d_{\text{Gap}}}{d_{\text{Threat-Threat}}} = \frac{d_{\text{Threat-Threat}} - r - R}{d_{\text{Threat-Threat}}} \tag{32}$$

where $d_{\text{Threat-Threat}}$ is the distance between the centers of two threats, d_{Gap} the shortest distance between two threats, r and R are the affecting radii of the two threats respectively. d_{Threat} is normalized within [0, 1]. The definition of threats distance is shown in Fig.3.

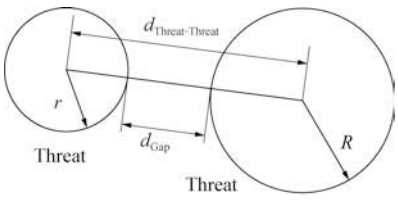

Fig.3 Definition of threats distance.

Redefine the fuzzy set of K, combine the middle K and small K to form a new small K while keep the large K invariable. Given the two proportion coefficients k_1 and k_2, the critical distance d_{Criti} between any two threats is computed according to Table 2.

Table 2 Fuzzy reasoning rules for critical distance

Rule number	Description
1	If k_1 is big and k_2 is big, then d_{Criti} is big
2	If k_1 is big and k_2 is small, then d_{Criti} is middle
3	If k_1 is small and k_2 is big, then d_{Criti} is middle
4	If k_1 is small and k_2 is small, then d_{Criti} is small

Compare the relationship between d_{Threat} and d_{Criti}, then the combination value V_{Cmb} will be

$$V_{\text{Cmb}} = \begin{cases} 1 & d_{\text{Threat}} \le d_{\text{Criti}} \\ 0 & d_{\text{Threat}} > d_{\text{Criti}} \end{cases} \tag{33}$$

Combine those whose V_{Cmb} equals 1 to form one group, and the process of grouping can be searched by the following adjacency matrix method.

First of all, we need to build the adjacent matrix $\boldsymbol{M}_{\text{Adj}}$, which is a square matrix and its dimension equals the number of threats. Elements in $\boldsymbol{M}_{\text{Adj}}$ are expressed by $\boldsymbol{M}_{\text{Adj}}[i][j] = V_{\text{Cmb}_{i,j}}$, where i, j represent the serial numbers of threats. Obviously, $\boldsymbol{M}_{\text{Adj}}$ is a symmetric matrix.

Search the adjacent matrix $\boldsymbol{M}_{\text{Adj}}$ and obtain the distribution of threats. The mth threat group can be expressed by the adjacency vector $\boldsymbol{V}_{\text{Adj}}[m]$. The nth element in $\boldsymbol{V}_{\text{Adj}}[m]$ can be represented by

$$\boldsymbol{V}_{\text{Adj}}[m][n] = \bigcup_{i=0}^{p-1} (\boldsymbol{M}_{\text{Adj}}[m][i] \times \boldsymbol{M}_{\text{Adj}}[i][n]) \tag{34}$$

where $\bigcup(\cdot)$ represents the logic operator "or", p the number of threats. Repeat the computation in Eq.(34) until $\boldsymbol{V}_{\text{Adj}}[m]$ is invariable. Those whose $\boldsymbol{V}_{\text{Adj}}[m][n]$ equals 1 are gathered into the mth group. The number of threat groups is the number of threats after combination.

Local minima in the path planning can be avoided by threats combination.

3.4. Flow of FVF path planning

The flowchart of the FVF path planning process is shown in Fig.4 where the three grey boxes represent three most significant components of the FVF method.

First of all, the initial conditions are input. Second, the step length of path planning is set according to Theorem 1 and the proportion coefficient k is set adaptively using the Bayesian belief network and fuzzy logic reasoning theories. The path planning process is executed, during which the combination of threats is called if local minima occurs. The path planning process continues until the destination is reached.

4. Simulation Results

In order to verify the effectiveness of the proposed UAV path planning approach based on FVF, simulations are conducted in a Visual C++ 6.0 programming environment on a PC with the following configurations: 32 b Intel Pentium IV processor with 3.00 GHz, 2 GB random access memory (RAM), and Windows XP operating system.

Simulations are carried out for the optimal solving method and the three components of FVF based path planning: the fixed step method, the adaptive parameter setting based on the Bayesian belief network and fuzzy logic reasoning theories, and the combination of threats.

Comparisons between the FVF method and the A* search algorithm are also presented below.

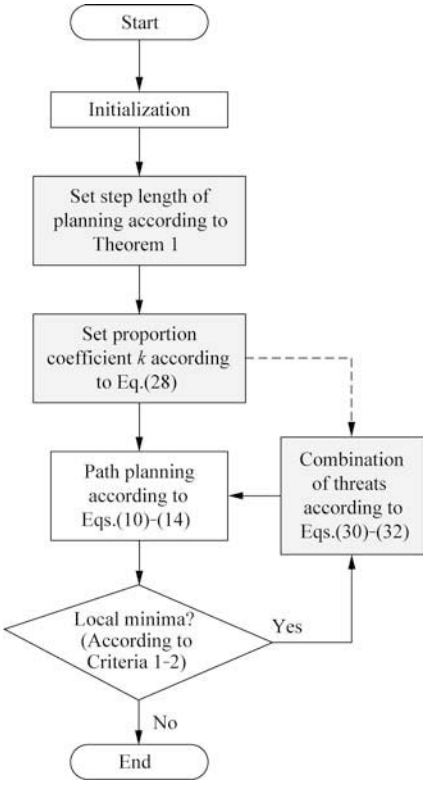

Fig.4 Flow chart of FVF path planning.

4.1. Comparisons between optimal solving method and fixed step method

Both the optimal solving method and the fixed step method have advantages and disadvantages. The following indicators are used to evaluate the performances of the two methods:

Indicator 1 Processing time (ProT).

Indicator 2 Path cost (PathC), which is computed according to Eq.(2).

Indicator 3 Path length (PathL).

Preset the starting point (5, 5) km, the destination (50, 50) km, the position, threat level and the impacted area of all seven threats.

The step length of the fixed step method is 100 m, namely, the planning gird is 100 m×100 m.

The planned paths by the two methods with respect to two scenarios are shown in Figs.5-6 and the corresponding performance indicators are listed in Table 3.

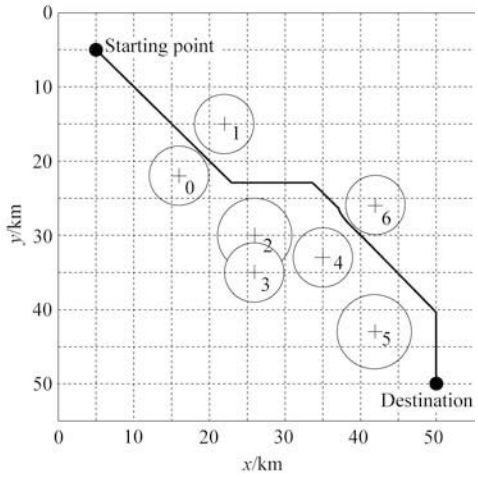

(a) Optimal solving method

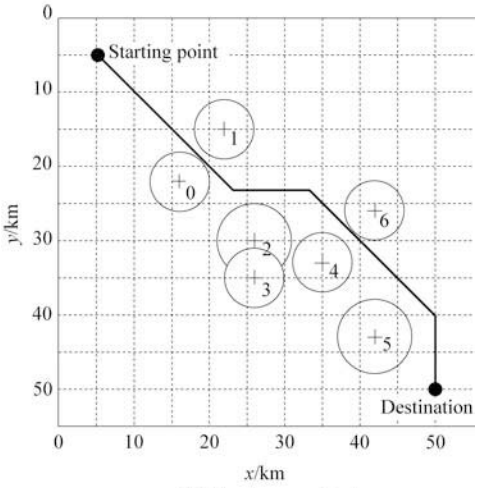

(b) Fixed step method

Fig.5 Path planned based on optimal solving and fixed step method in Scenario 1.

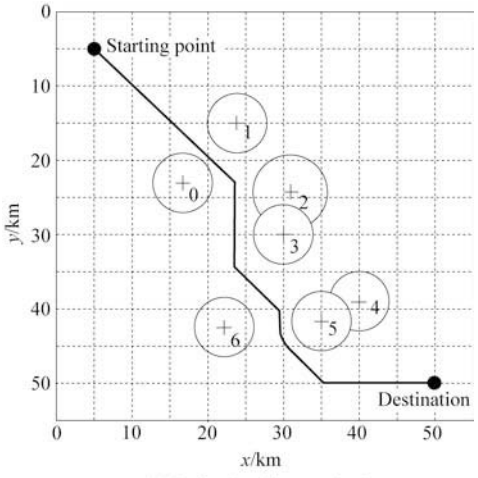

(a) Optimal solving method

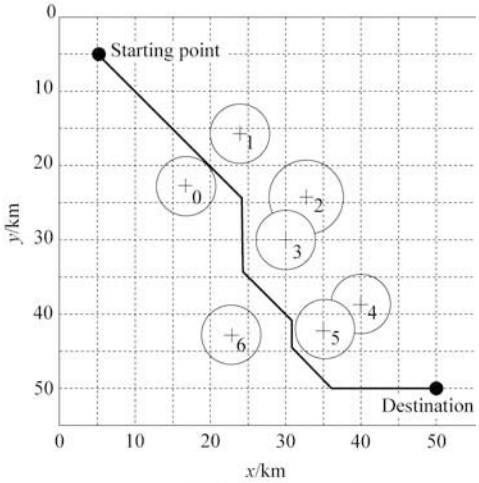

(b) Fixed step method

Fig.6 Path planned based on optimal solving method and fixed step method in Scenario 2.

Table 3 Performance indicators of optimal solving method and fixed step method

Method	Scenario 1		
	ProT/s	PathC	PathL/m
Optimal solving method	8.068 1	4.427 936 362	69 606
Fixed step method	0.048 7	4.433 336 362	69 663
Method	Scenario 2		
	ProT/s	PathC	PathL/m
Optimal solving method	9.502 1	4.600 241 296	72 314
Fixed step method	0.055 3	4.607 004 543	72 392

In Table 3, the processing time is computed by the counter values in PC.

From the simulation results above, it can be concluded that the path cost and path length of the optimal solving method is lower and shorter compared with the fixed step method, while the fixed step method has extreme short processing time. Therefore, the fixed step method adapts to the engineering application better and is suitable for UAV path planning.

4.2. Adaptive proportion coefficient

When PCL is weak (0.8) and TmR is low (0.3), the proportion coefficient k equals 1.5 according to the reasoning rules in Table 1. The planned path is illustrated in Fig.7(a). When PCL is strong (0.1) and TmR is high (0.8), we can obtain that k equals 0.6 and the planned path is shown in Fig.7(b).

From Fig.7, it can be concluded that when PCL is weak and TmR is low, the planned path is far from threats, or in other words, a safer path away from threats is chosen. When PCL is strong and TmR is high, in order to reach the destination as fast as possible, the threat cost is sacrificed in a reasonable range. Therefore the planned path goes through Threat 4 and Threat 5. Simulation results demonstrate that when the battlefield situation is varying, k changes adaptively.

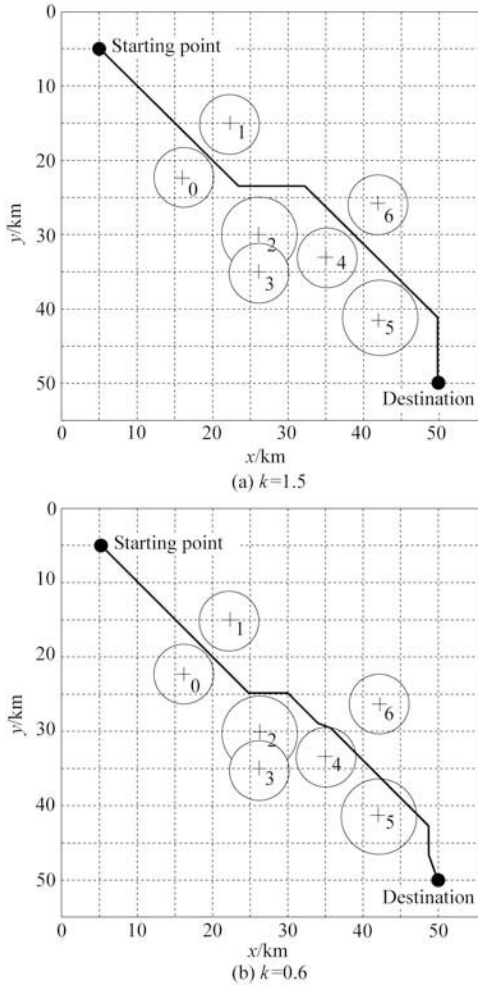

Fig.7 Path planned with different values of *k*.

4.3. Combination of threats

The combination of threats introduced in Section 3.3 is used to avoid local minima.

The simulation environment and the performance indicators defined are the same as those in Section 4.1. The initial conditions include starting point (5, 5) km, the destination (55, 60) km, the position, the threat level and the impacted area of all ten threats.

As shown in Fig.8(a), the planned path is trapped in a local minima area caused by concave distribution of virtual potential field constructed by Threats 4-9. The threats combination algorithm is used and we can obtain that the Threats 2-3 are grouped into one, so do the Threats 4-9. Re-plan the path based on combined threats and the result is shown in Fig.8(b).

In summary, simulation results show that:

(1) The combination of threats can solve the local minima problem effectively.

(2) The planned path not only avoids the concave distribution of threats but also shortens the path length and reduces the path cost.

The relationship between *k* and local minima is verified as follows.

As shown in Fig.9(a), when PCL is invariable and TmR is low, *k* is large and local minima exists; therefore, the path detours to reach the destination.

For the same problem, Fig.9(b) shows that when PCL is invariable and TmR is high, *k* is small and local minima does not exist; therefore, the path traverses through threats to reach the destination.

Simulation results in Fig.9 show that:

(1) When *k* is large and the critical distance is long, it is dangerous to traverse through the threats. In order to assure the safety, threats are combined and the corresponding path length is large.

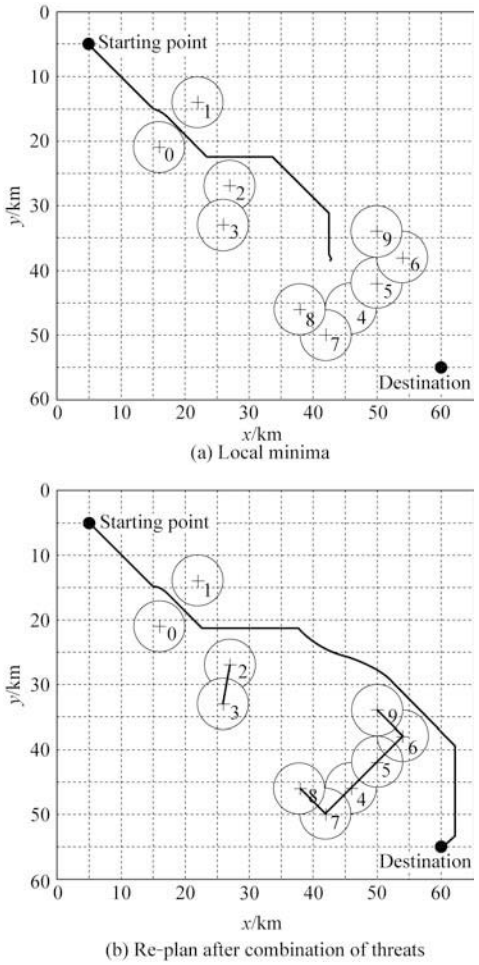

Fig.8 Threats combination to avoid local minima.

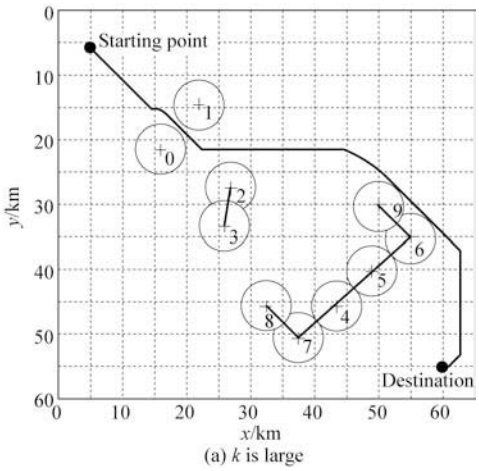

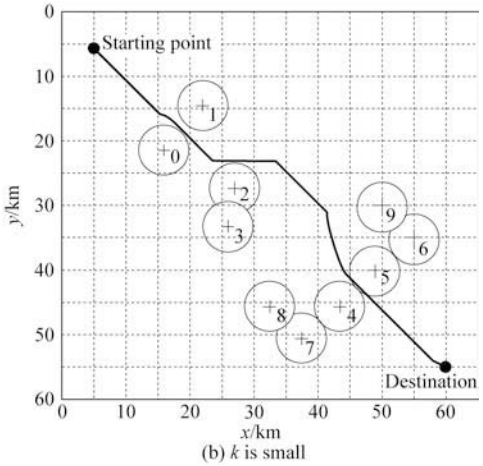

(b) k is small

Fig.9 Relationship between k and local minima.

(2) When k is small and the critical distance is short, the path can traverse through the threats to reach the given destination as fast as possible when necessary.

The local minima solution presented in this article gives the right way to traverse and detour for UAVs, so that the planned path is reasonable, flexible and can meet the requirements of different missions.

4.4. Comparisons between FVF method and A* search algorithm

In order to verify its usefulness in practice, the FVF method is compared with the A* search algorithm, which is widely used for UAV path planning.

The computational complexity of the A* search algorithm can be computed by

$$\Psi_{\mathrm{A}^*} = \eta N_{\mathrm{g}}^{\omega} \tag{35}$$

where N_{g} represents the number of grids, ω the dimension of path planning, η a coefficient which depends on the complexity of the environment. Meanwhile, the computational complexity of the FVF method is

$$\Psi_{\mathrm{FVF}} = \eta' \omega N_{\mathrm{g}} \tag{36}$$

where η' also represents a coefficient which depends on the complexity of the environment. It is obvious that the difference in computational complexities between these two methods grows larger when the path planning scale is bigger.

The simulation environment and the performance indicators defined are the same as those in Section 4.1. The initial conditions include starting point (5, 5) km, the destination (60, 60) km, the position, the threat level and the impacted area of all ten threats.

The step length of the FVF method is set to 100 m, and the grid of the A* search algorithm is set to the same size. The paths planned by the two methods with respect to two scenarios are presented in Figs.10-11, respectively. The corresponding performance indicators are listed in Table 4.

From the simulation results in this section, it can be concluded that the plan results by both methods are reasonable. The path cost and path length of the A* search algorithm is slightly lower and shorter, while the FVF method has much shorter processing time. In Scenario 1, the processing time of the FVF method is less than 1/5 of the processing time of the A* search algorithm. In Scenario 2, because of the local minima

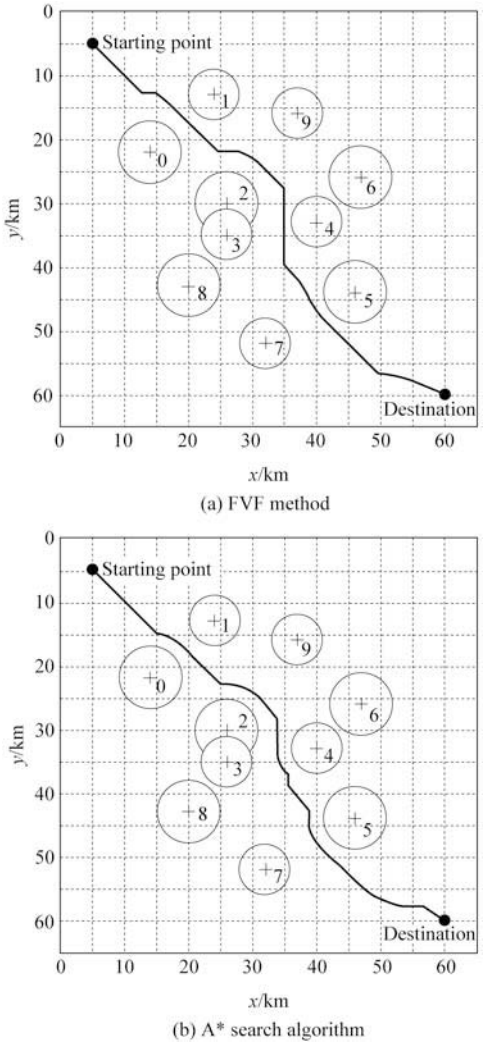

(a) FVF method

(b) A* search algorithm

Fig.10 Path planned based on FVF method and A* search algorithm in Scenario 1.

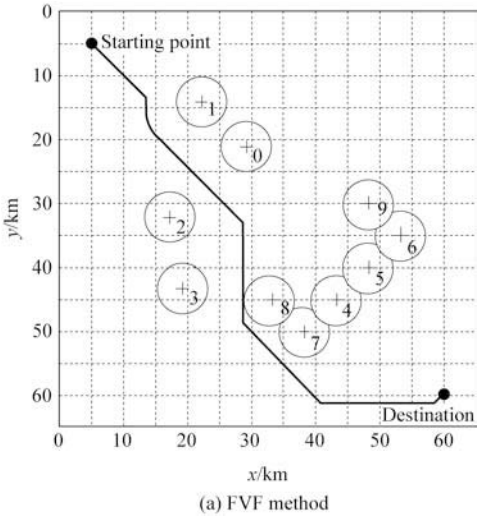

(a) FVF method

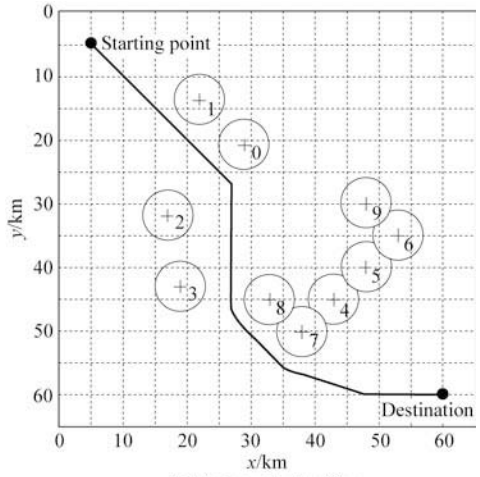

(b) A* search algorithm

Fig.11 Path planned based on FVF method and A* search algorithm in Scenario 2.

caused by the Threats 4-9, the processing time of FVF method is a little bit longer but still remarkably shorter than the A* search algorithm—it is about 1/3 of the A* search algorithm. Based on the simulation results, we can conclude that the FVF method meets the real-time requirements better.

Table 4 Performance indicators of FVF method and A* search algorithm

Method	Scenario 1		
	ProT/s	PathC	PathL/m
FVF method	0.020 9	6.690 557 933	86 217
A* search algorithm	0.110 9	6.689 239 861	86 048
Method	Scenario 2		
	ProT/s	PathC	PathL/m
FVF method	0.080 6	7.054 149 996	89 891
A* search algorithm	0.257 4	7.052 648 893	89 707

5. Conclusions

This article studies the UAV path planning approach based on FVF. The mathematical model of the path planning process is constructed using the hybrid system theory, and the corresponding optimal solution under the given indicators in path planning is presented.

To meet the real-time requirements of the online UAV path planning, a fixed step method is developed and the reachable condition is derived. The adaptive proportion coefficient based on the Bayesian belief network and fuzzy logic reasoning can adapt to the change of the battlefield situation. The combination of threats and the adjacent matrix are proposed to avoid local minima.

As illustrated in several examples, the FVF method is feasible and fast for UAV path planning. The comparisons between the FVF method and the A* search algorithm indicate that the FVF method is superior for the online UAV path planning in complicated environment.

The path planning approach in this article can be easily applied to three-dimensional space, and the computational complexity does not increase significantly. However, as three-dimensional path planning needs to consider the minimum of flying height, the maximum of climb angle and dive angle, etc., our future work will focus on this specific issue.

References

[1] Richards N D, Sharma M, Ward D G. A hybrid A*/ automaton approach to on-line path planning with obstacle avoidance. AIAA-2004-6229, 2004.

[2] Liu Z, Shi J G, Gao X G. Application of Voronoi diagram in flight path planning. Acta Aeronautica et Astronautica Sinica 2008; 29(S): 16-18. [in Chinese]

[3] Jennings A L, Ordonez R, Ceccarelli N. Dynamic programming applied to UAV way point path planning in wind. Proceedings of the IEEE International Symposium on Computer-Aided Control System Design. 2008; 215-220.

[4] Ye W, Ma D W, Fan H D. Algorithm for low altitude penetration aircraft path planning with improved ant colony algorithm. Chinese Journal of Aeronautics 2005; 18(4): 304-309.

[5] Kim Y, Gu D W, Postlethwaite I. Real-time path planning with limited information for autonomous unmanned air vehicles. Automatica 2008; 44(3): 696-712.

[6] Bottasso C L, Leonello D, Savini B. Path planning for autonomous vehicles by trajectory smoothing using motion primitives. IEEE Transactions on Control Systems Technology 2008; 16(6): 1152-1168.

[7] Yin L, Yin Y X. An improved potential field method for mobile robot path planning in dynamic environments. Proceedings of the IEEE International Conference on Intelligent Control and Automation. 2008; 4847-4852.

[8] Jaryani M H. An effective manipulator trajectory planning with obstacles using virtual potential field method. Proceedings of the IEEE International Conference on Systems, Man and Cybernetics. 2007; 1573-1578.

[9] Shi E X, Cai T, He C L, et al. Study of the new method for improving artifical potential field in mobile robot obstacle avoidance. Proceedings of the IEEE International Conference on Automation and Logistics. 2007; 282-286.

[10] Ding F G, Jiao P, Bian X Q, et al. AUV local path planning based on virtual potential field. Proceedings of the IEEE International Conference on Mechatronics and Automation. 2005; 1711-1716.

[11] Lee M C, Park M G. Artificial potential field based path planning for mobile robots using a virtual obstacle concept. Proceedings of the IEEE/ASME International Conference on Advanced Intelligent Mechatronics. 2003; 735-740.

[12] Chang Y C, Yamamoto Y. Dynamic decision making of mobile robot under obstructed environment. Proceedings of IEEE/RSJ International Conference on Intelligent Robots and Systems. 2006; 4091-4096.

[13] Dong Z N, Chi P, Zhang R L, et al. The algorithms on three-dimension route plan based on virtual forces. Journal of System Simulation 2009; 20(S): 387-392. [in Chinese]

[14] Alur R, Courcoubetis C, Henzinger T A, et al. Hybrid automata: an algorithmic approach to the specification and verification of hybrid systems, hybrid systems. Lecture Notes in Computer Science 1993; 736: 209-229.

[15] Pearl J. Probabilistic reasoning in intelligent systems: networks of plausible inference. San Francisco, CA: Morgan Kaufmann Publishers, Inc., 1998; 42-46.